Volume 131, Issue 5   May 2011   ISSN 0022-2313

AN INTERDISCIPLINARY JOURNAL OF RESEARCH ON
EXCITED STATE PROCESSES IN CONDENSED MATTER

JOURNAL OF LUMINESCENCE

EDITOR: R.S. MELTZER
DEPARTMENT OF PHYSICS AND ASTRONOMY
THE UNIVERSITY OF GEORGIA

ELSEVIER

Available online at www.sciencedirect.com
ScienceDirect

http://www.elsevier.com/locate/jlumin

Simulations of time-resolved photoluminescence experiments in α-Al₂O₃:C

Vasilis Pagonis [a,*], Reuven Chen [b], John W. Maddrey [a], Benjamin Sapp [a]

[a] McDaniel College, Physics Department, Westminster, MD 21157, USA
[b] Raymond and Beverly Sackler School of Physics and Astronomy, Tel-Aviv University, Tel-Aviv 69978, Israel

ABSTRACT

This paper presents simulations of time-resolved photoluminescence (TR-PL) experiments in α-Al₂O₃:C, which is one of the main dosimetric materials. During TR-PL experiments, short pulses of UV-light are followed by relaxation periods of the charge carriers. The model used in these simulations was previously used to explain radioluminescence (RL), thermoluminescence (TL) and photoluminescence (PL) experiments for this material, and is based on optical and thermal ionizations of excited *F*-centers. There are no published simulations of TR-PL experiments in this important dosimetric material in the literature. In this paper, we present new simulations using two slightly different versions of the model. In the first original version of the model, thermal quenching is explained via thermal ionization of the recombination centers. In the new proposed modified version of the model, thermal quenching is described by a Mott–Seitz type of mechanism, based on competitions between radiative and radiationless electronic transitions occurring within the recombination center. We simulate a typical TR-PL experiment in Al₂O₃:C at different stimulation temperatures, and compare the simulation results with available experimental data. It is found that both versions of the model provide a reasonable quantitative description of the luminescence lifetime and luminescence intensity as a function of the stimulation temperature. However, very significant differences between the two models are found for the behavior of the simulated integrated thermoluminescence (TL) and thermally stimulated conductivity (TSC) as a function of the heating rate used during such experiments. Only the results from the modified version of the model, (which is based on Mott–Seitz mechanism), are in good agreement with previously reported experimental results. The two models also predict very different behaviors for the dependence of the optically integrated stimulated luminescence (OSL) and TSC signals, as a function of the stimulation temperature. The results from the two models suggest that it may be possible to decide between the two mechanisms of thermal quenching in this material, by carrying out accurate measurements of the TL, TSC and OSL signals under different experimental conditions. The effect of shallow traps on the luminescence lifetimes is also studied and compared with available experimental data.

1. Introduction

The phenomenon of thermal quenching of luminescence from solids has been well-known for several decades (see, for example, reference [1], p. 44; and references therein). Thermal quenching manifests itself as a reduction of the measured luminescence intensity as the sample temperature is raised, and affects thermoluminescence (TL), optically stimulated luminescence (OSL), photoluminescence (PL) and radioluminescence (RL) experiments.

In addition to the well-known effects of thermal quenching on the luminescence intensity, thermal quenching also affects measurements of the luminescence lifetimes in α-Al₂O₃:C and other important dosimetric materials such as quartz [1–6]. Luminescence lifetimes can be measured during time-resolved photoluminescence (TR-PL) measurements. During such measurements, the stimulation and emission of luminescence is separated experimentally by using a short pulse of UV-light. This technique allows direct measurements of luminescence lifetimes and thus provides a means to estimate the delay between stimulation and emission of luminescence.

Thermal quenching phenomena in α-Al₂O₃:C have been the subject of several experimental studies, due to the importance of these effects in TL and OSL dosimetry [2,3,7,8]. In a seminal experimental study, Akselrod et al. [2] used time-resolved photoluminescence spectroscopy to measure the lifetime of the *F*-center luminescence from α-Al₂O₃:C within a wavelength range centered at 420 nm. They measured a lifetime of ∼35 ms at room temperature, decreasing to ∼2 ms at a stimulation temperature

of ~220 °C. These authors found that the decrease in the lifetime with stimulation temperature was described by an empirical Mott–Seitz type of expression characterized by an activation energy W and a dimensionless factor; this dimensionless factor was denoted by C in the work of Akselrod et al. [2], and by C′ in this paper. The values of these two parameters were confirmed by analyzing TL glow curves measured with different heating rates. An important finding of that study was that parameters C′ and W were independent of the glow curve shape, the degree of trap filling and of the specific conditions under which the crystals were grown. On the other hand, it was found that the photo-luminescence intensity depended on the sample type, the degree of trap filling, and the heating or cooling rate used during the TL experiments. Several of these experimental results were explained on the basis of phosphorescence signals originating in shallow TL traps present in the samples studied.

Thermal quenching in α-Al$_2$O$_3$:C has also been studied extensively using kinetic models (see, for example, [6,8–24]; and references therein). Vincellér et al. [22] summarized the two prominent theories of thermal quenching in α-Al$_2$O$_3$:C, namely Mott–Seitz mechanism and the alternative charge-transfer mechanism. In the former, the decrease of the luminescence efficiency is due to non-radiative transitions, whose probability increases with the sample temperature. This mechanism received strong experimental support by Akselrod et al. [2]. In the alternative charge-transfer mechanism proposed by Nikiforov et al. [18], thermal quenching is associated with a competition mechanism between recombination at F-centers and charge trapping at deep traps. Thermal and optical ionizations of F-centers are temperature dependent and play a key role in this alternative thermal quenching mechanism. The model has been used successfully to explain the results of several experiments on TL, thermally stimulated exoelectron emission, and thermally stimulated electrical conductivity ([13,14] and references therein).

Molnár et al. [21] investigated the influence of irradiation temperature on the TL peaks of α-Al$_2$O$_3$:C and confirmed the temperature dependence of the photoionization of F-centers. They noted that Mott–Seitz mechanism as well as the alternative charge-transfer mechanism leads to the same equation of the temperature dependence of the luminescence efficiency, and summarized the prevalent debate about which mechanism is dominant in this dosimetric material. By examining the dependence of the F^+-center emission on the heating rate, Vincellér et al. [22] proposed an energy band scheme, which involves three possible competitive pathways for thermally released charge carriers in this material.

There are no published simulations of TR-PL experiments for this important dosimetric material in the literature. In this paper, we present new simulations using two slightly different versions of the model developed by Nikiforov et al. [18]. In the first original version of the model, thermal quenching is explained via thermal ionization of the recombination centers. In the new slightly modified version of the model, thermal quenching is described by Mott–Seitz type of mechanism, based on competitions between radiative and radiationless electronic transitions occurring *within* the recombination center.

We simulate a typical TR-PL experiment in α-Al$_2$O$_3$:C at different stimulation temperatures, and compare the simulation results with the experimental results of Akselrod et al. [2]. It is found that both versions of the model provide a reasonably accurate quantitative description of the luminescence lifetime and luminescence intensity as a function of the stimulation temperature. However, the simulation results show that the integrated thermoluminescence (TL), integrated optically stimulated luminescence (OSL) and thermally stimulated conductivity

(TSC) have significantly different dependencies in the two models. It is found that only results from Mott–Seitz version of the model are in agreement with reported simultaneous measurements of TL and TSC. The results from the two models suggest that it may be possible to decide between the two mechanisms of thermal quenching in this material, by carrying out accurate simultaneous measurements of the TL, TSC and OSL signals under different experimental conditions. The effects of shallow electron traps (commonly found in this material) on the luminescence lifetime are also simulated, and the results of the simulation are compared with the experiment. Overall the results from the modified version of the model were found to be more consistent with the previously suggested Mott–Seitz mechanism of thermal quenching.

2. Mott–Seitz mechanism of thermal quenching in Al$_2$O$_3$:C

During TR-PL experiments in α-Al$_2$O$_3$:C, a brief pulse of UV stimulating light (205 nm) raises a small number of electrons into the conduction band (CB); these electrons will relax into the recombination center (RC). The relaxation probability $1/\tau$ will have contributions from radiative processes, from non-radiative transitions, and from phonon-assisted processes present in the material, and in general will be given by (Akselrod et al. [2], their Eq. (1))

$$\frac{1}{\tau} = \frac{1}{\tau_{rad}} + v \exp(-W/k_B T) + p \coth\left(\frac{\hbar \omega}{k_B T}\right), \qquad (1)$$

where τ_{rad} is the lifetime for the radiative recombination process, p is a temperature dependent constant, ω is the phonon vibration frequency, $\hbar$ is Planck's constant, v and W represent the frequency factor and the activation energy of the thermal quenching process, k_B is Boltzmann constant and T is the temperature of the sample (in K). The phonon contribution to τ from the last term in Eq. (1) is ignored in this paper, since there are currently no published studies of the effect of phonon coupling on the luminescence lifetimes in alumina. This paper represents a first attempt to incorporate the experimentally observed luminescence lifetimes within a kinetic model, and improved future versions of the model should include the strong phonon coupling effects which have been reported for this material (see, for example, Ref. [24]).

Eq. (1) leads to the temperature-dependent lifetime $\tau(T)$ of the form (Akselrod et al. [2], their Eq. (2))

$$\tau = \frac{\tau_{rad}}{1 + \tau_{rad} v \exp(-W/k_B T)} = \frac{\tau_{rad}}{1 + C' \exp(-W/k_B T)}, \qquad (2)$$

where the constant $C' = \tau_{rad} v$ is a dimensionless quantity. As the temperature T of the sample is increased during the optical stimulation, we expect the luminescence lifetime $\tau(T)$ to decrease according to Eq. (2).

A closely related phenomenon to the decrease of $\tau(T)$ with stimulation temperature T is the well-known decrease of the experimentally measured luminescence intensity $I(T)$ with stimulation temperature. Several experimental studies [2,6] have shown that the luminescence intensity $I(T)$ can also be expressed by the same thermal quenching factor as in Eq. (2)

$$I(T) = \frac{I_o}{1 + C' \exp(-W/k_B T)}, \qquad (3)$$

where I_o is the luminescence intensity at low temperatures, W represents as previously the activation energy for thermal quenching in α-Al$_2$O$_3$:C and C' is a dimensionless constant. Akselrod et al. [2] found that the radiative lifetime in α-Al$_2$O$_3$:C decreased in the temperature range 20–200 °C according to

Eq. (2) and were able to estimate the activation energy $W = (1.08 \pm 0.03)$ eV and the dimensionless constant $C' = (3.6 \pm 2.9) \times 10^{12}$. These authors also obtained an estimate of the luminescence lifetime at room temperature by averaging several samples; their average value was $\tau = (35 \pm 1)$ ms.

3. Description of the model of Nikiforov et al. [18]

Nikiforov et al. [18] developed a kinetic model which provides a description of the effect of thermal quenching on several luminescence phenomena in α-Al$_2$O$_3$:C. The detailed transitions in the model are shown in Fig. 1. The main feature of the model is a description of the thermal quenching mechanism, which is based on thermal and optical ionization of F-centers. In this paper, we use the same symbols and notation as in Nikiforov et al. [18], unless explicitly stated otherwise in the text.

In this model, the electron structure of F-centers in aluminum oxide is considered to be similar to the structure of a helium quasi-atom Evans [19]. The ground state is characterized by the ^1S level, while the excited states are considered to be a singlet (^1P) and a triplet (^3P) state. Excitation of an F-center corresponds to the $^1S \rightarrow {}^1P$ transition. The F-centers are thought to have excited states near the bottom of the CB. Excitation by UV-light at 205 nm leads to optical ionization of F-centers. As a result of this UV-stimulation, the concentration of F^+-centers grows with time.
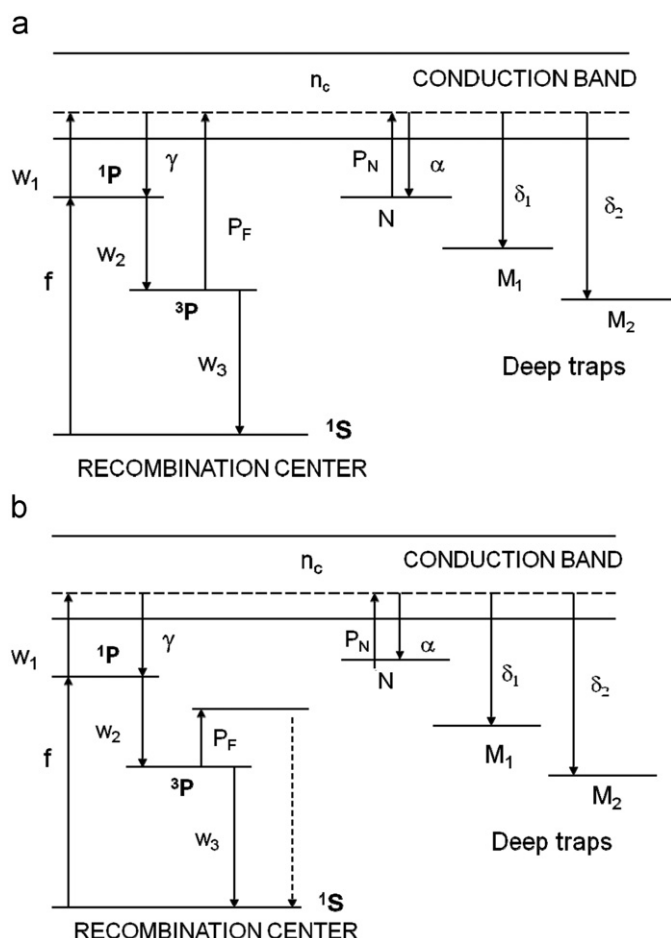
In Fig. 1, the symbols are as follows: N denotes the main dosimetric trap, M_1 and M_2 stand for deep electron traps, ^1P and ^3P are the excited levels of the F-center. Upon optical excitation in the absorption band, the center is excited to the ^1P state via the transition indicated by f in Fig. 1. Luminescence of an F-center (centered at ~420 nm) corresponds to the transition w_3 in Fig. 1. Thermal ionization of the F-center via the excited ^3P state corresponds to the transition indicated as P_F. The probability of thermal ionization of the excited ^3P state of the F-center is given by Boltzmann factor $P_F = C \exp(-W/kT)$, where W is the activation energy of the thermal quenching process and C is a frequency constant. Thermal ionization leads to a decrease in the fraction of radiative transitions (w_3) taking place at the center, and is believed to be the direct cause of thermal quenching of luminescence in this material. The optical transition denoted by w_1 results in the formation of an F^+ center according to $F^* - e = F^+$, while the F^+ center can change into an excited F-center upon capture of an electron according to $F^+ + e = F^*$. Free electrons from the ionization of F-centers can be captured in the dosimetric or deep traps.

The equations used in the model are as follows Ref. [18]:

$$\frac{dn}{dt} = -P_N n + \alpha(N-n)n_c, \tag{4}$$

$$\frac{dm_1}{dt} = \delta_1(M_1 - m_1)n_c, \tag{5}$$

$$\frac{dm_2}{dt} = \delta_2(M_2 - m_2)n_c, \tag{6}$$

$$\frac{dn_c}{dt} = P_N n - \delta_1(M_1 - m_1)n_c - \delta_2(M_2 - m_2)n_c - \gamma n_{F^+} n_c + P_F n_{3_P} \\ -\alpha(N-n)n_c + w_1 n_{1_P}, \tag{7}$$

$$\frac{dn_{F^+}}{dt} = P_F n_{3_P} - \gamma n_{F^+} n_c + w_1 n_{1_P}, \tag{8}$$

$$\frac{dn_{3_P}}{dt} = w_2 n_{1_P} - P_F n_{3_P} - w_3 n_{3_P}, \tag{9}$$

$$\frac{dn_{1_P}}{dt} = f + \gamma n_{F^+} n_c - w_1 n_{1_P} - w_2 n_{1_P}. \tag{10}$$

Here, N, M_1 and M_2 (cm^{-3}) denote the total concentration of dosimetric and deep traps; n, m_1, m_2, n_{1P} and n_{3P} (cm^{-3}) stand for the concentration of occupied levels in N, M_1, M_2, ^1P and ^3P, respectively; n_F^+ (cm^{-3}) is the concentration of F^+-centers; n_c (cm^{-3}) is the concentration of electrons in the conduction band; α, δ_1, δ_2 and γ (cm^{-3} s^{-1}) are the capture coefficients of carriers at the corresponding levels (Fig. 1); w_1, w_2 and w_3 (s^{-1}) denote the transition probabilities indicated in Fig. 1; f (cm^{-3} s^{-1}) is the excitation intensity. The transition probability w_1 is assumed to be independent of temperature, since the level ^1P is located near the bottom of the conduction band. The emptying probability for dosimetric traps is described by the expression $P_N = s \exp(-E/kT)$, where E is the trap depth of the main dosimetric trap and s is the corresponding frequency factor.

In addition to the above equations, the model also ensures the conservation of charge at all times via the equation

$$n + m_1 + m_2 + n_c = n_{F^+}. \tag{11}$$

The instantaneous luminescence I_L from the radiative recombination center is defined as

$$I_L = w_3 n_{3_P}. \tag{12}$$

The original values of the parameters in the model of Nikiforov et al. [18] are as follows: $E = 1.3$ eV, $s = 10^{13}$ s^{-1}, $\alpha = 10^{-14}$ cm^3 s^{-1}, $\delta_1 = 10^{-12}$ cm^3 s^{-1}, $\delta_2 = 10^{-14}$ cm^3 s^{-1}, $\gamma = 10^{-11}$ cm^3 s^{-1},

Fig. 1. (a) Schematic diagram of the model by Nikiforov et al. [18], which contains a dosimetric trap N and two deep electron traps indicated by M_1 and M_2. The various transitions and the parameters used in the model are described in the text. (b) The modified energy scheme proposed in this paper, which follows closely the description of thermal quenching using Mott–Seitz mechanism.

$N=10^{13}$ cm^{-3}, $M_1=10^{14}$ cm^{-3}, $M_2=10^{14}$ cm^{-3}, $w_1=1$ s^{-1}, $w_2=10$ s^{-1}, $w_3=1$ s^{-1} and $f=10^{10}$ cm^{-3} s^{-1}.

These values of the kinetic parameters were used in the earlier work by Milman et al. [6] to describe specific features of TL in this material (such as the quenching parameters, transition probability and concentration of traps). The same numerical values were also used by Nikiforov et al. [18] to calculate the temperature dependence of the intensity of photo- and radioluminescence under different occupancy of the deep traps in the model. Variables used in the model were the temperature and the occupancy of deep traps, expressed in terms of the variable ratios m_{10}/M_1 and m_{20}/M_2. The model showed that thermal quenching becomes less efficient when the deep traps are occupied, in agreement with experimental observations.

In the absence of experimental evidence to the contrary, we will assume that the dominant luminescence process, during the TR-PL experiment, is the slow transition from the metastable ^3P state into the ground state ^1S shown in Fig. 1, and that this transition gives rise to the experimentally observed lifetime of $\tau=35$ ms at room temperature. The rest of the kinetic processes shown in Fig. 1 are assumed to take place much faster, within characteristic times of 1 ms or less; transition w_1 is assumed in the original model of Nikiforov et al. [18] to take place slower, according to its assigned numerical value of $w_1=1$ s^{-1}. However, the value of this parameter did not significantly affect the results of the simulations presented in this paper.

In order to obtain quantitative agreement between the model and the TR-PL experiments of Akselrod et al. [2], it was found necessary to change three of the parameters in the model, namely the values of w_3, w_2 and M_1. Firstly, in order to match the experimentally observed lifetime of $\tau=35$ ms at room temperature, the value of the transition probability w_3 from the metastable ^3P state into the ground state was changed to $w_3=1/\tau=1/(35\text{ ms})=29$ s^{-1}, from its original value of $w_3=1$ s^{-1}. Secondly, it was found necessary to change the transition probability w_2 from level ^1P to level ^3P to a much larger value of $w_2=3\times10^3$ s^{-1}. This change was necessary so that the electronic transition $1P\rightarrow3P$ takes place quickly within the model during and after the UV-pulse, on a time scale of <1 ms. Finally, we adjusted the concentration of electrons in the electronic trap M_1 from a value of $M_1=10^{14}$ cm^{-3} into a larger value of $M_1=10^{15}$ cm^{-3}. This last change was necessary so that the conduction band also quickly empties when the UV-pulse is turned off, within a time scale of <1 ms. The rest of the parameters in the model were left unchanged. The thermal quenching parameters C' and W were treated as adjustable parameters within the model, and their values were adjusted to get the best possible fit to the experimental data of Akselrod et al. [2]. The initial conditions for the different concentrations are taken to be zero, unless otherwise indicated in results of the simulations. The system of differential Eqs. (4)–(10) was solved using the software package *Mathematica*. By varying the parameters of the model, it was found that the thermal quenching process depends critically on the kinetic parameters w_3, C' and W. The thermal quenching properties seem to be much less sensitive to changes made to the rest of the parameters in the model.

4. The modified version of the model

We propose the new slightly modified version of the model of Nikiforov et al. shown in Fig. 1b. In this version of the model, the transition P_F of Fig. 1a does not raise electrons into the conduction band, but rather raises them into an excited state within the recombination center as shown in Fig. 1b. From this excited energy level, the charge carriers are removed by radiationless transitions into the ground state, shown by a vertical dashed line in Fig. 1b. The details of this radiationless transition are not important for purposes of the numerical simulations. What is important is (a) the existence of this competing radiationless mechanism and (b) that the electrons taking part in these transitions are not raised into the conduction band. It is important to note that this newly proposed energy scheme is also more consistent with experimental data available on the energy differences between levels ^1P, ^3P and ^1S in this material, as follows. The ^1P state has been reported to be below or inside the conduction band, and ~6 eV above the ^1S ground state. In addition, the ^3P state is ~3 eV (wavelength of ~420 nm) above the ^1S state; this energy difference describes the photon energy emitted during the well-known F-center $^3P\rightarrow^1S$ transition. The expected energy difference between ^1P and ^3P states is therefore about 3 eV, which is in agreement with the representation of the states drawn in Fig. 1. However, this value of 3 eV is in disagreement with the experimental value for the thermal quenching activation energy $W\sim1.1$ eV reported by several authors. This discrepancy in the activation energy value W could possibly be explained by invoking a two-stage transition mechanism, which eventually could raise the electrons from the level ^1P into the conduction band. The first thermally activated stage with energy W, could perhaps be followed by a second such stage, which raises the electrons into the conduction band. An alternative possibility for this second stage could be a hopping type of mechanism assisted by band-tail states located between the conduction band and the ^1P state.

Instead of invoking such a double-transition mechanism, we propose the slightly modified version of the model shown in Fig. 1b. This slightly different energy scheme provides an alternative mechanism for thermal quenching in this material. It is noted that the proposed new energy scheme in Fig. 1b is very similar to the original mechanism shown in Fig. 1a, hence the essential nature of the original model is not altered significantly by the proposed changes. However, the thermal quenching mechanisms in the two versions of the model are very different. The new energy scheme in Fig. 1b describes the thermal quenching process as a completely *internal* mechanism within the recombination center. While in Fig. 1a, the electrons are raised by process P_F into the CB, electrons participating in the non-radiative transitions P_F in Fig. 1b are completely removed from the charge carriers transferred through the conduction band. Thus, in principle thermal quenching effects described by the two models of Fig. 1a and b, should produce very different experimental behaviors.

In the new scheme shown in Fig. 1b, Eqs. (4)–(12) in the model remain the same, with the exception of Eqs. (7) and (8). Eq. (7) is now modified as follows:

$$\frac{dn_c}{dt} = P_N n - \delta_1(M_1-m_1)n_c - \delta_2(M_2-m_2)n_c - \gamma n_{F^+} n_c - \alpha(N-n)n_c + w_1 n_{1_P}.$$

(7a)

In this modified form of the equation, the term $+P_F n_{3_P}$ is absent, indicating the fact that electrons are not raised into the conduction band from level ^3P, but rather are raised thermally into an excited state of the recombination center, from which they subsequently undergo a radiationless transition into the ground state. Similarly Eq. (8) will be modified by removing the term $+P_F n_{3_P}$ resulting in the following expression:

$$\frac{dn_{F^+}}{dt} = -\gamma n_{F^+} n_c + w_1 n_{1_P}.$$

(8a)

It is noted that the proposed scheme in Fig. 1b is completely analogous to our recently proposed quantitative thermal quenching kinetic model for quartz, which is based on Mott–Seitz

mechanism Pagonis et al. [20]. In this proposed scheme for quartz, thermal quenching arises by the competition between radiative and non-radiative electronic transitions taking place within the recombination center. One main difference between thermal quenching mechanisms in quartz and α-Al$_2$O$_3$:C is the very different value of the luminescence lifetime at room temperature: in alumina the metastable state displays a luminescence lifetimes of ~35 ms, while in unannealed quartz typical luminescence lifetime values are almost three orders of magnitude smaller, with a numerical value of ~42 µs.

5. Simulation of a typical TR-PL experiment

We have simulated a typical TR-PL experiment in which the UV-stimulation is initially ON for 0.2 s and is subsequently turned OFF for the same length of time. During the OFF part of the simulation, the optical excitation parameters f and w_1 are set equal to zero. The initial concentration of electrons in the deep trap M_1 were taken to be $m_{10} = 10^{14}$ cm^{-3}. From Eq. (11), this results in an initial concentration of F^+ centers equal to $(n_{F+})_0 = m_{10} = 10^{14}$ cm^{-3}. Fig. 2 shows results of this simulation using the models in Fig. 1a and b, and with parameters listed in a previous section. Both versions of the model gave the same results. The decaying part of the signal in Fig. 2 is fitted to a single decaying exponential plus a constant, while the rising part of the signal in the same figure is fitted to a saturating exponential function plus a constant. The fits are shown as lines through the simulated data in Fig. 2, and they yield similar luminescence lifetimes with values $\tau_{rise} = (31 \pm 0.1)$ ms and $\tau_{decay} = (32 \pm 0.1)$ ms.

We have repeated this simulation by varying the stimulation temperature in the range 20–300 °C, with results shown in Figs. 3–5. The solid line in Figs. 4 and 5 shows results from both versions of the model. Fig. 4 shows clearly that as the stimulation temperature increases, the luminescence lifetime obtained from both the rising and falling parts of the signals in Fig. 3 shows a continuous decrease with the stimulation temperature, due to the presence of thermal quenching. The luminescence lifetimes τ are obtained by fitting the simulated TR-PL curves in Fig. 3 to single exponential functions. In some simulations presented later in this paper for samples containing thermally shallow electron traps, it is necessary to use exponential functions plus a constant. As pointed out by Akslerod et al. [2], this constant represents
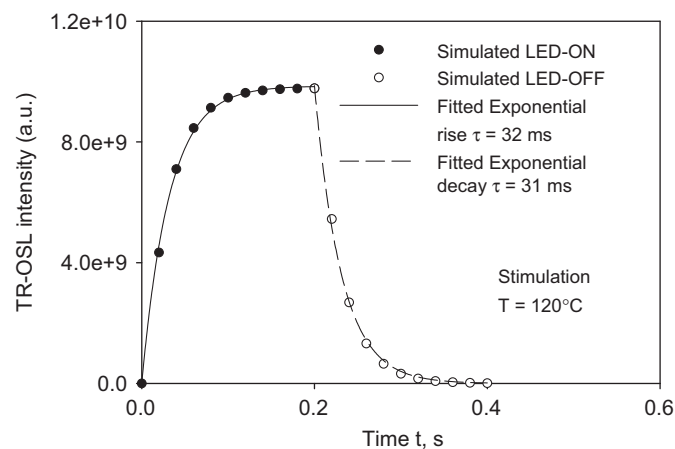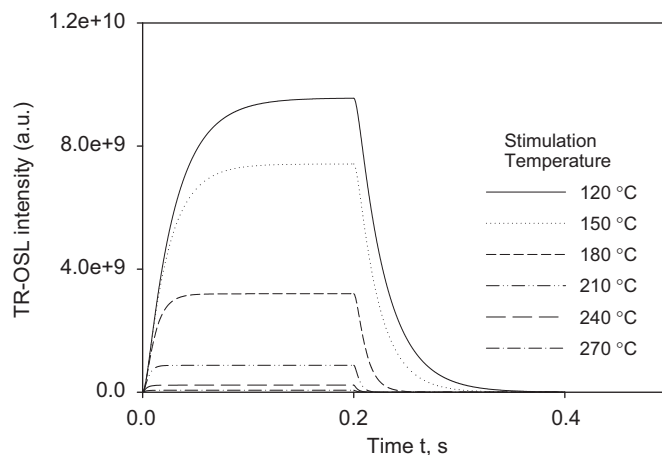

Fig. 3. Simulated time resolved spectra at various stimulation temperatures between 20 and 300 °C. As the stimulation temperature increases, the corresponding luminescence lifetime and the luminescence intensity decrease for both parts of the signal.
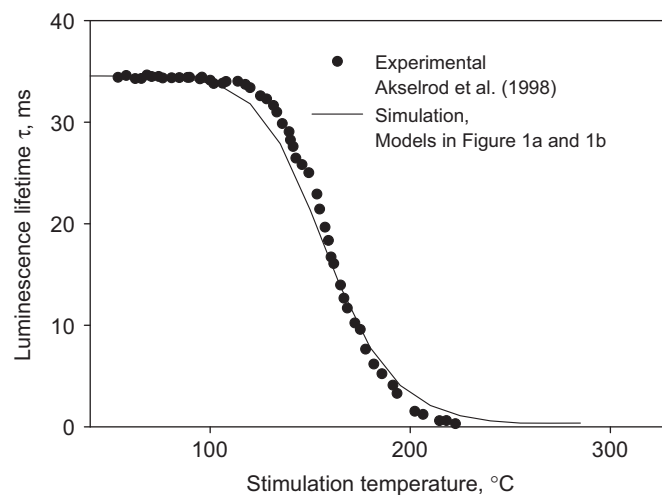

Fig. 4. The luminescence lifetimes τ obtained by fitting single exponentials to the simulated TR-PL curves in Fig. 3 (solid line). The same results are obtained using both models in Fig. 1a and b. Superimposed on the simulated data, we show the corresponding experimental data from Akselrod et al. [2] as solid circles.
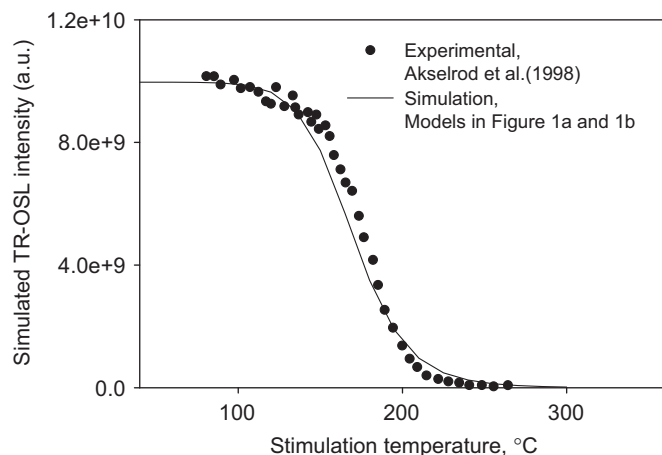

Fig. 2. Simulated time resolved spectrum for α-Al$_2$O$_3$:C using the model shown in Fig. 1a. The UV-stimulation is ON for 0.2 s and OFF for the same amount of time. The rising and decaying parts of the signal are fitted with a rising exponential plus a constant and a decaying exponential plus a constant correspondingly, yielding the luminescence lifetime τ values of $\tau_{rise} = (31 \pm 0.1)$ ms and $\tau_{decay} = (32 \pm 0.1)$ ms for the two parts of the signal.

Fig. 5. Integrated TR-PL intensity of the simulated signals shown in Fig. 3 as a function of the stimulating temperature (solid line). The same results are obtained using both models in Fig. 1a and b. Superimposed on the simulated data, we show as solid circles the corresponding experimental data from Akselrod et al. [2], their Fig. 3a for sample #1.

phosphorescence from various traps during measurement of the luminescence signal. The simulated results in Fig. 4 show that as the stimulation temperature increases, the luminescence lifetime obtained from the exponential fits shows a continuous decrease from ~35 to ~1 ms in the temperature range 20–240 °C. It is noted that the rising and decaying parts of all simulated TR-PL signals in Fig. 3 yield the same luminescence lifetimes, in agreement with the results of several previous experimental studies in quartz and α-Al$_2$O$_3$:C [4,17].

Superimposed on the simulated data of Fig. 4, the experimental luminescence lifetime τ is shown as solid circles from Akselrod et al. [2], their Fig. 2. The simulated data in Fig. 4 was fitted using the thermal quenching Eq. (2). The best-fit parameters C' and W obtained from the simulated data in Fig. 4 were $W=1.0$ eV, $C'=1.2\times10^{13}$. These values of the thermal quenching parameters are in reasonable agreement with the broad limits of $W=1.08\pm0.03$ eV and $C'=(3.6\pm2.9)\times10^{12}$ established by Akselrod et al. [2] from averaging many different samples. Fig. 5 shows the integrated TR-PL intensity of the simulated signals shown in Fig. 3, as a function of the stimulating temperature (solid line). Superimposed on the simulated data, the corresponding experimental data are shown as solid circles from Akselrod et al. [2], their Fig. 3a for sample #1. Once more, it was found that both versions of the model provide a reasonable fit to the experimental data, and they produce the same results. The simulated data is obviously not in complete agreement with the experimental data, but the agreement can be considered as reasonable, considering the fact that we are using a rather simplistic model in order to describe a very complex luminescence mechanism in this material. Furthermore, in this paper, we are more interested in drawing general comparisons between the two models, in order to possibly provide modeling support for one thermal quenching mechanism over the other.

In the next section, we carry out simulations of TL, TSC and OSL measurements in this material using both versions of the model, and compare simulated results with experimental data. It will be shown that only results from the modified version of the model are in agreement with the experimental data, and hence results in this paper provide support for Mott–Seitz mechanism in α-Al$_2$O$_3$:C.

6. Simulations of TL, TSC and OSL experiments

Fig. 6 shows the results of simulating simultaneous TL and TSC measurements carried out with different heating rates, by using the *original* version of the model in Fig. 1a. Fig. 7 shows the corresponding simulated results for the *modified* version of the model. The quantities TL and TSC shown in these figures are obtained by integrating the TL and TSC curves over the complete temperature range of the heating process, namely 20–300 °C. A linear heating rate is simulated instead of the brief UV-pulse, and therefore the parameter f in Eq. (10) is set equal to zero during simulations. In addition, the initial concentration of electrons in the dosimetric trap is taken as $n_0=10^{12}$ cm^{-3}. The system of differential Eqs. (4)–(12) is now solved using a constant linear heating rate β, so that the temperature of the sample depends on time according to $T=T_o+\beta t$, where $t=$time (s), $T=$temperature (K), $T_o=$room temperature (K) and $\beta=$heating rate in K/s. The heating rate in the simulations of Figs. 6 and 7 is varied from 0.5 up to 4 K/s.

The five curves shown in Figs. 6 and 7 were calculated by using different degrees of filling of the deep traps (M_1 in Fig. 1), from a relatively low trap filling ratio of $m_{10}/M_1=0.30$ (30% of saturation level), to an almost completely filled trap ratio of $m_{10}/M_1=0.95$ (95% of saturation level). Figs. 6a and 7a show
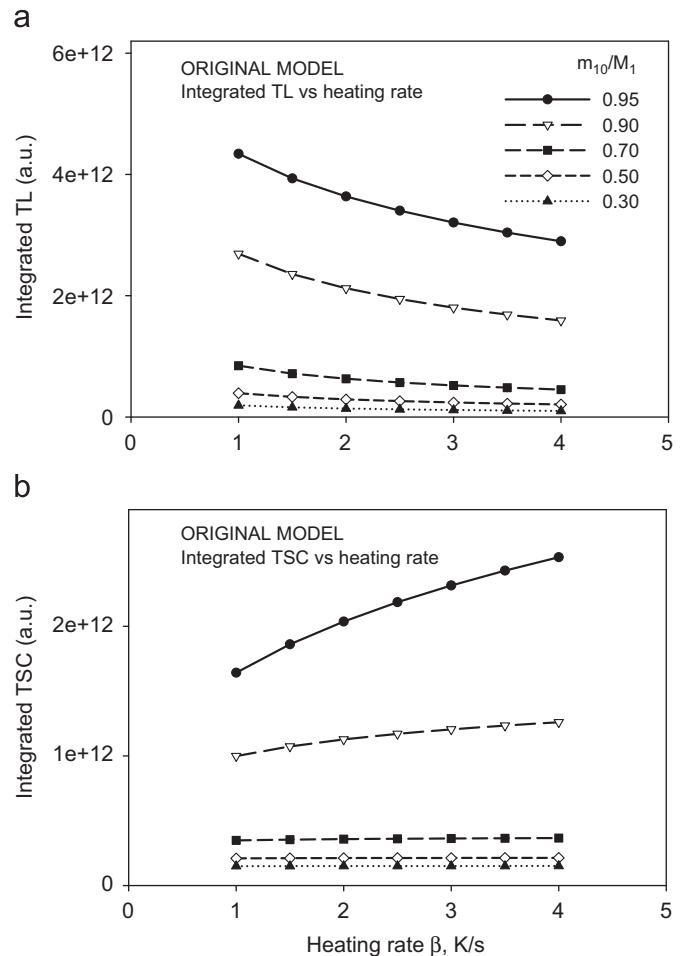

Fig. 6. The simultaneous integrated (a) TL and (b) TSC signals as functions of the heating rate, simulated using the original model of Fig. 1a. The five simulated curves shown were obtained using different amounts of filling of the deep traps, by changing the ratio m_{10}/M_1.

that as the heating rate is increased during a simulated TL experiment, the TL intensity in both versions of the model shows the same behaviors, namely it decreases as the heating rate is increased, as expected due to thermal quenching of the luminescence intensity. The situation is very different when comparing the behavior of the TSC signals in Figs. 6b and 7b. While in the original model, there is a continuous increase of the TSC signal with the heating rate, in the modified version of the model the TSC intensity is independent of the heating rate. Only the results from the modified Mott–Seitz type model are in very good agreement with the experimental results of Akselrod et al. [2], their Fig. 6. By contrast, the original thermal ionization model in Fig. 1a fails to produce the experimentally observed constant TSC signal as a function of the heating rate. In addition, as the degree of filling of the deep traps m_{10}/M_1 is increased in Fig. 6a, thermal quenching effects become more significant in the original version of the model.

In Figs. 8 and 9, we show simulated results for simultaneous continuous-wave (CW-OSL) and photostimulated conductivity (PSC) experiments carried out at different stimulation temperatures, using both models. A constant-intensity OSL illumination intensity is simulated (CW-OSL), in which trapped electrons are optically evicted from the dosimetric trap. In these simulations the system of Eqs. (4)–(12) remains unchanged, with only one important change: the thermal excitation probability term $P_N=s\exp(-E/kT)$ in Eqs. (4) and (7), is replaced by the corresponding optical
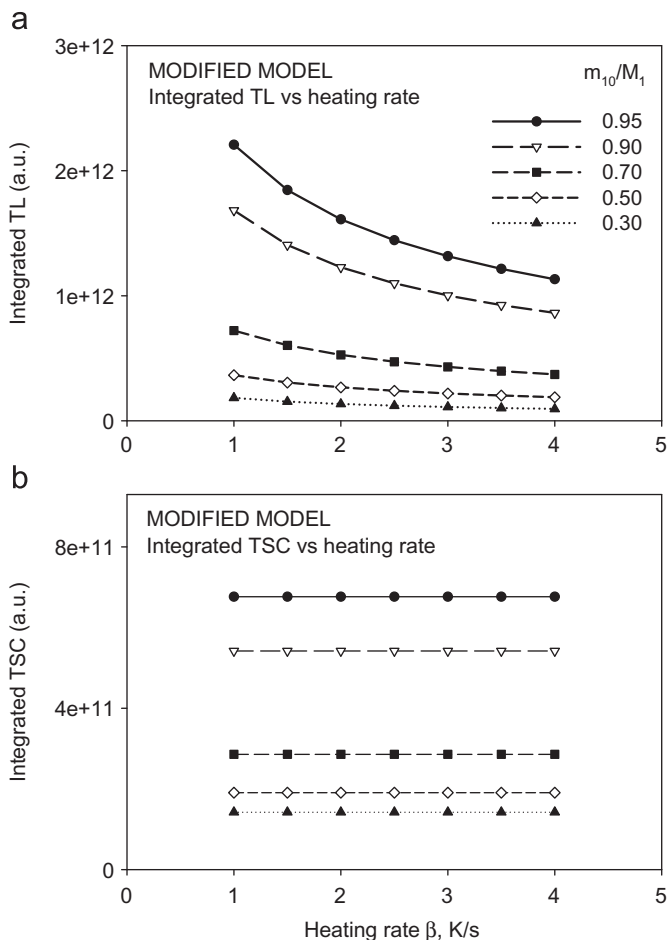
Fig. 7. Same as Fig. 6, but using the modified model of Fig. 1b.

Fig. 8. The simultaneous integrated (a) OSL and (b) PSC signals as functions of the heating rate, simulated using the original model of Fig. 1a. The five simulated curves shown were obtained using different amounts of filling of the deep traps, by changing the ratio m_{10}/M_1.

excitation probability $P_N = \lambda$. The optical excitation probability $P_N = \lambda$ is assigned a numerical value of $\lambda = 0.1\,\mathrm{s}^{-1}$ in the simulations; the results of the simulation do not depend on the numerical value of λ.

Both models show similar dependence of the integrated OSL signal in Figs. 8a and 9a, with the shape of these curves representing the effect of thermal quenching. However, significant differences between the two models can be seen clearly at high stimulation temperatures. The integrated OSL signal for the top curve in Fig. 8a becomes zero at a stimulation temperature of $\sim 300\,°C$, while the corresponding signal in Fig. 9a reaches zero at a much earlier temperature of $\sim 250\,°C$. This difference between the two versions of the model can be explained as follows. Transition P_F in Fig. 1a raises electrons into the conduction band, while the same electronic transition in Fig. 1b removes electrons which would otherwise take part in the luminescence process. As a result of the difference between the transition P_F in the two models, the integrated OSL signal in Fig. 8a decays slower than the corresponding signal in Fig. 9a, as the stimulation temperature is increased.

The situation is dramatically different when comparing behaviors predicted from the models in Figs. 8b and 9b. As in the case of the TL/TSC simulations shown in Figs. 6 and 7, comparison of Figs. 8b and 9b shows that results from the two models indicate very different behaviors as a function of the stimulation temperature. In the modified version of the model, the PSC intensity is independent of the stimulation temperature (Fig. 9b); while in the original model, the integrated PSC depends very strongly on both the stimulation temperature and on the
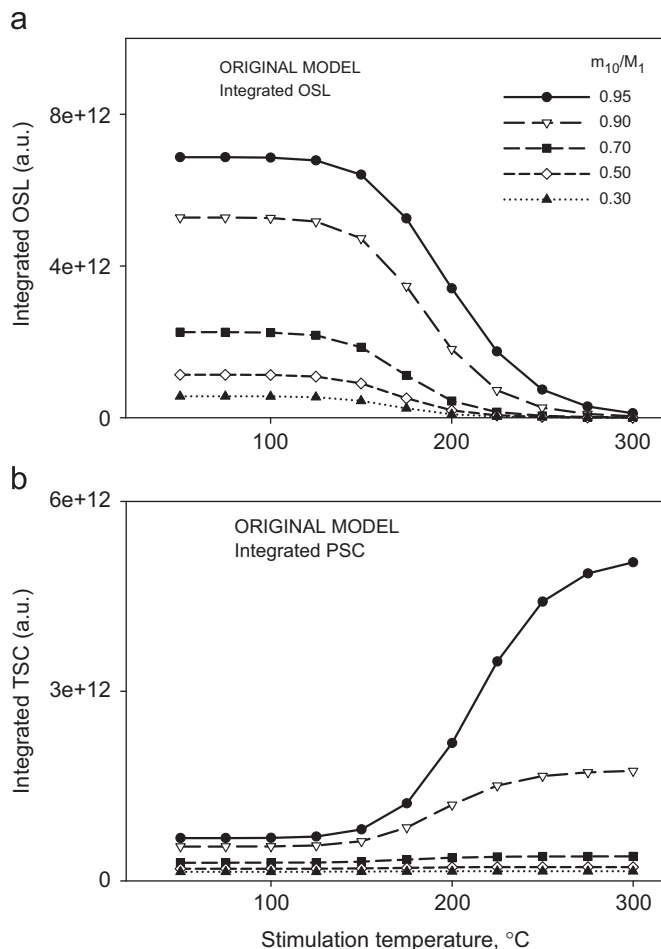
degree of filling of the traps (Fig. 8b). To the best of our knowledge, this type of simultaneous OSL and PSC experiment has not been reported in the literature, and we propose it as a possible way to distinguish between the two models of thermal quenching.

It is noted that the phenomena shown in Figs. 8 and 9 for higher stimulation temperatures are rather complex, involving both thermal and optical processes. This is likely to make the interpretation of experimental data more complicated.

In the next section, we simulate the effect of thermally shallow traps on the luminescence lifetime at various stimulating temperatures; the simulated results are compared with the experimental data of Akselrod et al. [2].

7. The effect of thermally shallow electron traps on the luminescence lifetimes

Akselrod et al. [2] showed that the presence of thermally shallow electron traps can affect the shape of the TR-PL decay curves, and can therefore lead to increased experimental luminescence lifetimes τ at low temperatures. These authors found that as the electrons are released from shallow traps while heating the sample, the measured lifetime increased from 35 ms to a maximum value of ~ 63 ms at about 50 °C, and subsequently gradually decreased to the values expected from Eq. (2).
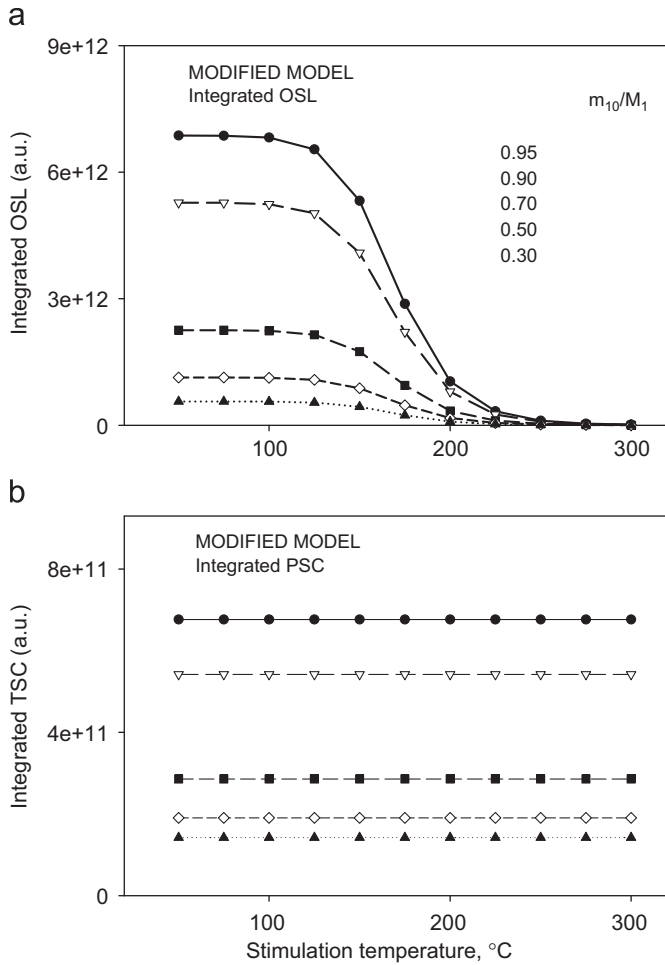
a

b

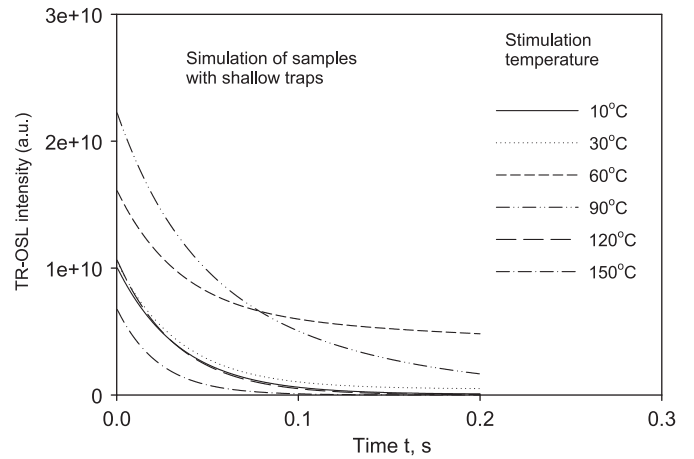Fig. 9. Same as Fig. 8, but using the modified model of Fig. 1b.

Fig. 10. Simulated TR-PL decay curves at different stimulation temperatures, when the shallow electron traps are included in the model.
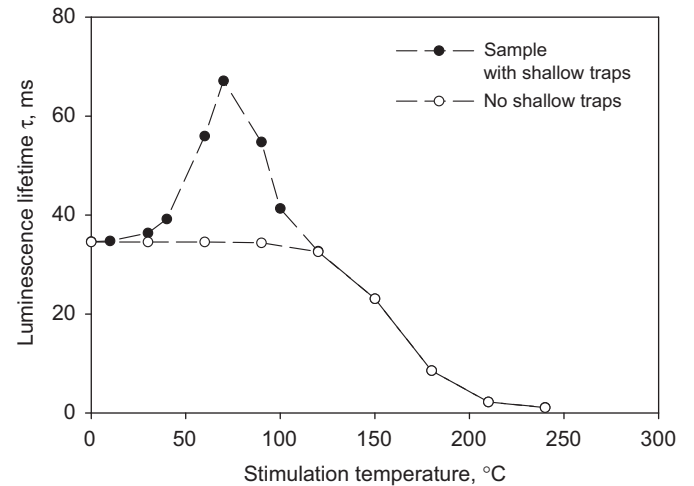

Fig. 11. The calculated lifetimes obtained by fitting single exponentials to the initial part of the curves of Fig. 6, as a function of the stimulation temperature. This figure is to be compared with the experimental results shown in Akselrod et al. [2], their Fig. 2.

We have simulated this effect by adding such a shallow electron trap to the model. Mathematically the inclusion of the shallow traps in the model is accomplished by adding the following equation to describe the thermally unstable shallow trap

$$\frac{dn_{sh}}{dt} = -s_{sh}\exp(-E_{sh}/k_BT)n_{sh} + A_{sh}(N_{sh}-n_{sh})n_c, \qquad (13)$$

where n_{sh} and N_{sh} represent the instantaneous and total concentrations of electrons in the shallow traps. In the usual notation, s_{sh} and E_{sh} represent the frequency factor and activation energy for electrons in the shallow trap, while A_{sh} represents the probability of retrapping. The first term in the sum in Eq. (13) represents the thermal release of electrons from the shallow trap into the CB, while the second term in this equation represents the probability of retrapping of electrons into the shallow trap. Eqs. (7) and (11) were also modified appropriately by including appropriate terms representing the effects of the shallow trap. The values of the kinetic parameters used to describe the thermally shallow trap were chosen as $s_{sh} = 10^{13}\,s^{-1}$ and $E_{sh} = 0.9\,eV$. These values correspond to a typical low temperature TL peak in this material at $\sim 65\,°C$, when measured with a heating rate $\beta = 4\,K/s$. The initial concentration of the shallow traps was taken as $n_{sh}(0) = 0.55 \times 10^{12}\,cm^{-3}$ and the total concentration as $N_{sh}(0) = 5.5 \times 10^{12}\,cm^{-3}$, while the value of the retrapping coefficient was taken as $A_{sh} = 10^{-10}\,cm^3\,s^{-1}$.

Figs. 10 and 11 demonstrate the effect of adding a shallow trap to the model. Fig. 10 shows some of the simulated TR-PL decay curves when the shallow electron traps are included in the model; at low stimulation temperatures, the decay curves decrease much slower with time than the corresponding curves in Fig. 3. Fig. 11 shows the corresponding calculated lifetimes by fitting the initial part of the TR-PL decay curves in Fig. 10 to exponentials plus a constant. The results in Fig. 11 are similar to the experimental data of Akselrod et al. [2], their Fig. 2, which show a very similar increase of the apparent lifetime at low temperatures. The calculated lifetime for these shallow traps using the first order kinetics expression $\tau = s^{-1}\exp(-E/kT)$ yields the following values: $\tau \sim 11\,s$ at $50\,°C$, with the lifetime decreasing gradually to a value of $\tau \sim 0.8\,s$ at a temperature of $75\,°C$, and $\tau \sim 35\,ms$ at $120\,°C$.

Similar results to the ones shown in Fig. 11 were obtained for these simulations by using the modified version of the model in Fig. 1b. We conclude that both versions of the model can provide a description of these experimental results.

8. Conclusions

In this paper, two versions of the kinetic model of Nikiforov et al. [18] were used to simulate typical TR-PL experiments in α-Al$_2$O$_3$:C. It was found that both versions of the model can

V. Pagonis et al. / Journal of Luminescence 131 (2011) 1086–1094

provide reasonable quantitative agreement with published values of the luminescence lifetime at different stimulation temperatures. The effect of shallow traps on the luminescence lifetimes was also studied using the simulations, and was found to be in qualitative agreement with the experimental work of Akselrod et al. [2].

In the original version of the model, thermal quenching is explained on the basis of photoionization and thermal ionization of F-centers. Competition between the two transitions w_3 and P_F shown in Fig. 1a leads to a reduced luminescence intensity, as well as a decreased luminescence lifetime at higher stimulation temperatures. In this paper, we proposed the slightly different version of the model shown in Fig. 1b, which follows closely the original description of thermal quenching mechanism by Mott and Seitz. This type of competition mechanism between non-radiative and radiative transitions in Mott–Seitz model for α-Al$_2$O$_3$:C is very similar to our recently published model of thermal quenching for quartz Pagonis et al. [20].

Using the two versions of the model, important differences were found for the simulated behavior of the integrated thermoluminescence (TL), integrated optically stimulated luminescence (OSL) and thermally stimulated conductivity (TSC). Only the results from the modified version of the model (which is based on Mott–Seitz mechanism), are in good agreement with reported experimental results. The simulations presented here suggest that it may be possible to decide between the two mechanisms of thermal quenching in this material, by carrying out accurate measurements of the TL, TSC and OSL signals under different experimental conditions.

Acknowledgements

References

[1] L. Bøtter-Jensen, S.W.S. McKeever, A.G. Wintle, Optically Stimulated Luminescence Dosimetry, Elsevier, Amsterdam, 2003.
[2] M.S. Akselrod, N. Agersnap Larsen, V. Whitley, S.W.S. McKeever, J. Appl. Phys. 84 (1998) 3364.
[3] M.S. Akselrod, N. Agersnap Larsen, V. Whitley, S.W.S. McKeever, Radiat. Prot. Dosimetry 84 (1999) 39.
[4] M.L. Chithambo, J. Phys. D.: Appl. Phys. 40 (2007) 1874.
[5] M.L. Chithambo, J. Phys. D.: Appl. Phys. 40 (2007) 1880.
[6] I.I. Milman, V.S. Kortov, S.V. Nikiforov, Radiat. Meas. 29 (1998) 401.
[7] G. Kitis, Phys. Status Solidi (A), Appl. Res. 191 (2002) 621.
[8] V.H. Whitley, S.W.S. McKeever, J. Appl. Phys. 87 (2000) 249.
[9] J.C. Polf, E.G. Yukihara, M.S. Akselrod, S.W.S. McKeever, Radiat. Meas. 38 (2004) 227.
[10] L.E. Colyott, M.S. Akselrod, S.W.S. McKeever, Radiat. Prot. Dosimetry 65 (1996) 263.
[11] Agersnap Larsen, N., 1999. Ph.D. Thesis, Risø National Laboratory, Roskilde, Denmark. Available online at: ⟨http://www.risoe.dk/rispubl/NUK/ris-r-1090.htm⟩.
[12] N. Agersnap Larsen, L. Bøtter-Jensen, S.W.S. McKeever, Radiat. Prot. Dosimetry 84 (1999) 87.
[13] V.S. Kortov, I.I. Milman, S.V. Nikiforov, Radiat. Prot. Dosimetry 84 (1999) 35.
[14] V.S. Kortov, I.I. Milman, S.V. Nikiforov, E.V. Moiseĭkin, Phys. Solid State 48 (2006) 447.
[15] J.M. Edmund, C.E. Andersen, Radiat. Meas. 42 (2007) 177.
[16] V. Pagonis, R. Chen, J.L Lawless, Radiat. Meas. 42 (2007) 198.
[17] V. Pagonis, S.M. Mian, M.L. Chithambo, E. Christensen, C.J. Barnold, Phys. D: Appl. Phys. 42 (2009) 055407.
[18] S.V. Nikiforov, I.I. Milman, V.S. Kortov, Radiat. Meas. 33 (2001) 547.
[19] B.D.J. Evans, J. Nucl. Mater. 219 (1996) 202.
[20] V. Pagonis, C. Ankjærgaard, A.S. Murray, M. Jain, R. Chen, J. Lawless, S. Greilich, J. Lumin. 130 (2010) 902.
[21] G. Molnar, M. Benabdesselam, J. Borossay, P. Iacconi, D. Lapraz, M. Akselrod, Radiat. Prot. Dosimetry 100 (2002) 139.
[22] S. Vincellér, G. Molnar, K. Berkane, P. Iacconi, Radiat. Prot. Dosimetry 100 (2002) 79.
[23] A. Berkane-Krachai, P. Iacconi, R. Bindi, S. Vincellér, J. Phys. D: Appl. Phys. 35 (2002) 1895.
[24] D.R. Mishra, M.S. Kulkarni, K.P. Mutheb, C. Thinaharan, M. Roc, S.K. Kulshreshtha, S. Kannand, B.C. Bhatt, S.K. Gupta, D.N. Sharma, Radiat. Meas. 42 (2007) 170.